Insights into the CO_2 Reduction Pathway Through the Electrolysis of Aldehydes on Copper

Research Thesis

Presented in partial fulfillment of the requirement for graduation with honors research distinction in Chemistry in the undergraduate College of Arts and Sciences of The Ohio State University

By Benjamin P. Charnay

The Ohio State University

April 2021

Advisor: Professor Anne C. Co

Department of Chemistry and Biochemistry

Abstract

The use of fossil fuels throughout the modern world has resulted in an alarming increase in atmospheric carbon dioxide concentrations (now >400 ppm at Mauna Lua). As a result, promising technologies which can aid in the development of carbon neutral fuel cycles or energy storage are in high demand. One promising candidate is electrochemical CO_2 reduction which offers the promise of targeted conversion of CO_2 to value-added or fuel-like chemicals at atmospheric temperatures and pressures. This can offer an exciting utilization avenue for captured CO_2 which is widely discussed nowadays. In order for this technology to become useful at scale the development of a robust, efficient, and selective catalyst is a requirement. Understanding of the CO_2 reduction pathway can provide guidance for rational catalyst design capable of maximizing the overall effectiveness of novel catalysts. In this work we study the proposed step of acetaldehyde to ethanol by utilizing ^{13}C labeled acetaldehyde as a feed stock and monitoring produced ethanol via NMR. A similar approach was taken to analyze propionaldehyde conversion to 1-propanol. This work also provided theoretical and experimental arguments for copper's unique ability to catalyze this reaction.

Acknowledgements

To the Co Group, my family, my friends. Without whom none of this would have been possible. I am always grateful.

Contents

1. Background

1.1 Climate Change and the Greenhouse Effect

Since the onset of fossil fuel combustion for energy at the start of the industrial revolution, atmospheric carbon dioxide concentrations have been increasing exponentially[1]. The greenhouse effect of gasses in the atmosphere is most certainly instrumental in allowing surface conditions on earth to be tolerable to life, but it has become common knowledge in recent years that carbon concentrations as high as they currently are, can have catastrophic ramifications. It is worth noting that in the past, CO_2 concentrations in the atmosphere may have been much higher than now and life persisted, the obvious difference being the extreme rate of changed caused by anthropogenic emissions does now allow for adaptation and evolution by flora and fauna which has already resulted in the 6^{th} mass extinction event on the planet.

The greenhouse effect caused by certain gasses in the atmosphere is named after the produce growing method, and behaves in a similar way. The temperature of the earth is maintained in a careful balance based on an equilibrium of absorbed and emitted radiation. Higher energy radiation makes it through the atmosphere and hits the earth which absorbs the energy and re-emits longer wavelength radiation. This IR radiation makes its way back into space unless absorbed by IR active molecules, greenhouse gasses. These absorbing molecules absorb and reemit the radiation in no specific direction, meaning some of the IR is bounced right

back towards the earth. This 1-way mirror effect results in overall higher average temperatures of the atmosphere and surface. Gases are compared according to the global warming potential

	Relative global warming potential	
Gas	**20 years**	**100 years**
CO_2	1	1
CH_4	56	21
N_2O	280	310
CFC-11	4360	1900

(GWP) agreed to in the Kyoto Protocol, where CO_2 was assigned a GWP of 1.

Table 1. Relative Global Warming Potential of some greenhouse gasses

There do exist a number of natural carbon sinks, namely oceans and plant life. Oceans dissolve carbon dioxide according to Henry's Law and a number of equilibrium steps. This equilibrium results in an overall lower pH and Ocean Acidification, though discussion of this effect is outside the scope of this thesis. The other natural sink is surface greenery, namely rainforests and algae. Algal life is negatively affected by the aforementioned acidification, and land-based forests are being destroyed by human behavior.

1.2 Electrochemical CO_2 Reduction

As a means of addressing the increasing CO_2 concentrations in the atmosphere and mediating the resulting ramifications, carbon capture and sequestration have emerged as potentially powerful tools. Direct electrocatalytic conversion of CO_2 was studied to a great depth by Hori et al. who grouped metals based on their ability to produce different products from CO_2

reduction. Copper immediately emerged as a particularly intriguing metal for its ability to produce fuel-like chemicals in the form of methane and a number of alcohols. Later, Kuhl et al. identified 16 distinct products which can be formed from the reduction of CO_2 on copper.

Direct CO_2 conversion has been likened to synthetic photosynthesis (when photovoltaics are the energy source) or reverse combustion. These are both apt metaphors as CO_2 is indeed reduced hydrocarbons/oxygenates. Each reaction has a known reduction potential which reflects the thermodynamic change from the reactants to the products which one would imagine is the potential needed to undergo the conversion to that reaction.

Half-reaction	E^0 **(V)**
$CO_2 + H_2O + 2e^- \rightarrow CO + 2OH^-$	-0.11
$CO_2 + H_2O + 2e^- \rightarrow HCOO^- + OH^-$	-0.02
$CO_2 + 5H_2O + 6e^- \rightarrow CH_3OH + 6OH^-$	0.03
$CO_2 + 6H_2O + 8e^- \rightarrow CH_4 + 8OH^-$	0.16
$2CO_2 + 5\ H_2O + 8e^- \rightarrow CH_3COO^- + 7\ OH^-$	0.12
$2CO_2 + 9H_2O + 12e^- \rightarrow C_2H_5OH + 12OH^-$	0.08
$2CO_2 + 8H_2O + 12e^- \rightarrow C_2H_4 + 12OH^-$	0.07
$2CO_2 + 10H_2O + 14e^- \rightarrow C_2H_6 + 14OH^-$	0.14
$3CO_2 + 13H_2O + 18e^- \rightarrow C_3H_7OH + 18OH^-$	0.09

Table 2. Common carbon dioxide reduction half-reactions and their standard reduction potentials referenced to SHE at pH 0.31[2]

In practice, each of these reactions has an activation energy much higher than the standard reduction potential, this is known as overpotential. Specifically, the overpotential is defined as the amount of voltage required to achieve a given current density (commercial electrocatalysts can operate at 200 mA/cm^2). As such these reactions require substantially more energy to proceed. A catalyst served the role of lowering this activation energy. The lowering of

onset potential is the first figure of merit needed when evaluating a catalyst and can be measure simply.

As can be seen from the huge diversity of products copper is capable of producing, selectivity is also a key metric when discussing catalysts. It is in this domain where detailed understanding of reaction mechanism is most crucial. The most desirable products of CO_2 reduction require 12 or more electrons, involving a huge number of elementary steps. A useful catalyst must be able to guide the intermediates along this path to result in very high selectivity. According to the Sabatier Principle, "in order to have high catalytic activity, the interaction between reactants and catalysts should neither be too strong nor too weak. If the interaction is too weak, then there will be no reaction on the surface because it is difficult for catalyst surface to bind the reactants. If the interaction is too strong, then the reaction reactant or product is difficult to get desorbed from catalyst surface, which also lowers the activity"[3]**.** In a process with as many steps as reducing CO_2 to ethanol, any intermediate may be the "key" whose binding energy defines the overall catalytic performance, and as such a sophisticated understanding of the mechanism is necessary if an advanced catalyst is to be developed. A plot of binding energy vs. activity has come to be known as a "volcano plot" owing to its mountainous shape.

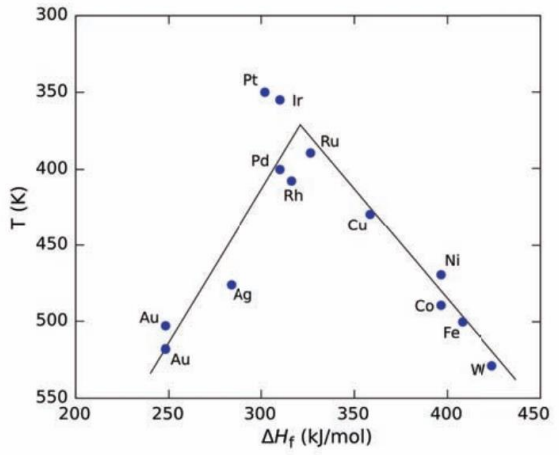

Figure 1. An example of volcano plot, showing the rate of decomposition of formic acid on transition metal surfaces

Some materials such as gold naturally have high selectivity (>90% for CO), but the higher value products will require more advanced catalysts. This thesis will focus on the analysis of one particular proposed step in the mechanism towards ethanol with the goal of providing additional evidence for this step and a means of testing other proposed steps in a robust and simple manner. Additional work has been done evaluating a parallel path to 1-propanol.

1.3 Analytical Techniques Employed

1.31 GC/MS, GC-TCD:

Analysis of the gaseous products of CO_2 reduction as described in subsequent sections was performed through a combination of Gas Chromatography-Mass Spectrometry and Gas Chromatography-Thermal Conductivity Testing. The separatory technique in both cases is the same, a gas chromatograph which separates the product gas flow by different physical properties (based on the properties of the column).

Gas chromatography functions by carrying sample gasses via a carrier gas, the mobile phase, through a long column. The affinity for different gasses to pass through the column more or less easily causes the different gasses to separate in time before they meet the detector. In this case the detector is either a quadrupole mass spectrometer or a thermal conductivity detector.

The mass spectrometer operates by differentiating mass charged fragments of analyte gasses by mass-to-charge ratio. The thermal conductivity detector is a hot filament which has a resistance based on the atmosphere it is surrounded by, monitoring this current allows for identifying the change in makeup of gasses passing over the filament.

1.32 NMR

Nuclear Magnetic Resonance, NMR, was performed to quantify liquid products and to track the conversion of isotopically labeled samples. Put simply, NMR functions by coupling a collection of NMR susceptible nuclei (n* ½) to a large external magnetic field. A pulsed radio frequency causes the net magnetization vector of all of the nuclei to become perpendicular to the detector (a coil of wire known as a Faraday Detector). As the resonance decays (return to randomization, a vector parallel to the detector) the moving dipole moment generates a current in the detector which is measured as signal.

For this research, specific implementation of analytic techniques is discussed in further detail in the methods section.

2. Introduction

Atmospheric carbon dioxide is at an all-time high[1], which invites new technology to address this emerging crisis. A possible solution is a carbon-neutral fuel cycle, where the product of fossil fuel combustion, CO_2, is converted back to a fuel using renewable sources of energy. Moreover, a liquid fuel, such as alcohols, are advantageous[4] as they utilize existing liquid energy storage infrastructure in addition to their higher heating value. The electrochemical reduction of CO_2 (CO2RR) is a technology that can fulfill this role[5–10]. The CO2RR technology has been known of and experimented with since the 80's[9,10]; Hori demonstrated copper's unique ability to generate many organic products including small alcohols. Research in this area has primarily been on the development of selective electrocatalysts to form complex hydrocarbons from CO_2, aided with theoretical studies suggesting plausible mechanistic routes[11–22]. A better understanding of reaction pathways can facilitate the design of an effective catalyst with a higher degree of product selectivity. Despite extensive literature on CO2RR, many aspects of the mechanism on

heterogenous catalysts surfaces is still unclear. As such, experimental evidence which can prove or disprove a proposed pathway is highly desirable.

It is widely acknowledged that CO is a key reaction intermediate for the formation of hydrocarbons[1,5,22]. The reduction of CO generally leads to hydrocarbons similar to those produced from the electroreduction of CO_2[9,23]. Calculations have shown that the dimerization of adsorbed CO_{ads}, can lead to C-C formation on Cu(100) at low overpotentials[20,21,24,25]. On Cu (211), this activation barrier was found to be very high[21]. Cross-coupling of CO and acetaldehyde was also shown to form precursors to propanol[26]. Several works have also suggested reactions between CHO_{ads} and CO_{ads} leads to C-C on Cu(100)[27,28]. The formation of C-C, while an extremely important step, is relatively early on a mechanistic path towards C2, C3, and C4 species observed in experiments. Once C-C bond is formed, several pathways still exist, leading to a range of products[18]. As such, a reaction pathway that leads to a specific molecule, such as ethanol, is still unclear and much debated.

In this work, we study the reduction of small molecules that appear in the proposed mechanistic pathway of CO_2. We first identify molecules that are the end products, where they can no longer be further reduced on a catalyst surface. Next, we identify "stable" molecules, that sometimes appear in trace amounts in the reported literature, and determine if they can be further reduced, herein referred to as intermediates of CO_2 reduction. In this thesis, we focus on the proposed final steps to the formation of alcohols, through the reduction of aldehydes.

Similar strategies have been previously reported with very interesting results[29,30]. Schouten et al. investigated the reduction of intermediates and confirm the reduction of formaldehyde to methanol, ethylene oxide to ethylene, glyoxal and glycoaldehyde to acetaldehyde and ethanol.

Glycoaldehyde was found to also produce butanediol, while C4 species were not observed on glyoxal reduction[29]. Furthermore, they stated several end products that are not further reduced on Cu, such as methanol and oxalic acid. Kuhl et al.[5] and Ledezma-Yanez et al.[31] had also reported the detection of acetaldehyde and ethanol during CO_2 reduction on Cu(111).

This work takes a similar approach to deconvolute the potential pathways to the formation of ethanol. We had previously determined that methanol, ethanol, propanol, and formic acid are not further reduced on copper electrodes (at < 1.4 V vs. RHE). These molecules are referred to as the end products. Herein, we focus on the electrochemical reduction of aldehydes, such as acetaldehyde and propanal, on polycrystalline Cu, to illustrate their viable pathway to ethanol and 1-propanol, respectively. Trace amounts of acetaldehyde and propanal are sometimes reported in the literature as a minor product during CO_2 reduction, suggesting active sites or active interfacial regions on the catalysts leading to aldehyde formation and that these aldehydes maybe further reduced to from an alcohol end product.

$$C_2H_4O + 2\ e^- + 2\ H^+ \text{ à } C_2H_5OH \qquad (1)$$

We also show that chemical conversion of aldehydes to alcohols over a copper catalyst, in the absence of an applied bias, is not observed, even at elevated temperatures. Furthermore, we report that this two electron and two proton reduction process occurs on Cu but not Au. Consequently, while the reaction step involving the reduction of aldehyde may not be the limiting step in the overall reduction of CO_2, the selective reduction observed on Cu suggests that the role of the

catalyst, especially for complex multistep reactions, can be more complicated beyond influencing the slowest step in the overall reaction.

3. Experimental Methods

3.1 Electrode Preparation

The working electrode, polycrystalline copper foil (Sigma-Aldrich, 99.99%), was cut to the appropriate size (8 cm × 4.5 cm × 0.5 mm). Prior to every experiment, the copper electrode was electropolished in 85% phosphoric acid (Fischer Scientific, certified ACS) at an oxidation potential of ca. 1.7 V vs Ag/AgCl (Biologic VSP potentiostat) for 5 min. The actual oxidation potential was determined for each foil by performing a linear sweep voltammogram in 85% phosphoric acid solution. The polishing potential used was positive of the Cu oxidation peak and before water oxidation. After electropolishing, the foil was then rinsed thoroughly in deionized water (Milli Q, Advantage A10) with a total organic count of < 2 ppb, dried with nitrogen gas, and vacuum sealed until used as the working electrode.

Gold electrodes were prepared by first polishing aluminum and stainless-steel plates (8 cm x 4.5 cm x 0.5 mm) with a 0.5 um alumina slurry (Buehler Company) until almost mirror finish, then sonicated (three times 10 s each) in acetone, methanol and deionized water. Cleaned and polished aluminum and stainless-steel plates were sputter-coated with Au (Denton, 99.999%) for 5 minutes to 1000-2000 Å.

3.2 Solution Preparation

The electrolyte solution was prepared from diluting a 2 M stock solution of $KHCO_3$ (Fischer Scientific, USP/FCC grade) in deionized water with an organic count under 2 ppb (18.2 MΩ, Milli-Q, Advantage A10). The 2 M $KHCO_3$ stock solution was electrolyzed at 2.0 V, at approximately 5 mA/cm^2, for 24 h using a dimensionally stabilized anode (DSA®, de Nora) as the electrode. The pre-electrolyzed solution was diluted to 0.1 M with deionized water.

The aldehyde solutions were prepared from concentrated solutions (Sigma-Aldrich 99%) and diluted to 50 mL at a concentration of 2500 ppm (0.0567 M) and 5000 ppm (0.114 M) for natural abundance acetaldehyde, labeled acetaldehyde, and propionaldehyde respectively using deionized water.

3.3 Electrochemical Cell

Experiments were conducted using a three-electrode assembly at room temperature and ambient pressures. The cell was custom made from acrylic and consisted of two compartments, working and counter, separated by Selemion AMV anion exchange membrane (AGC Engineering Co.) and sealed with Viton gaskets. The cell was kept in deionized water and cleaned thoroughly with fresh deionized water (18.2 MΩ) prior to assembly. The electrolyte was a 0.1 M solution of $KHCO_3$ saturated with CO_2. The counter electrode consisted of a sheet of dimensionally stabilized anode (DSA) and the reference electrode was a reversible hydrogen electrode (RHE), created by flowing H_2 over a platinized Pt gauze in 0.1 M $KHCO_3$ solution (pH 9.2) in a separate compartment with a Luggin capillary. All of the potentials reported are referenced against RHE at the same pH as the working electrode compartment (pH of 6.8 in a 0.1 M $KHCO_3$). The geometric surface area of both the working and counter electrode was 26 cm^2. The electrolyte was saturated prior to

electrolysis with CO_{2re}, bringing its pH to 6.8. The electrolyte was then flowed through the cell at a rate of 3 mL/min. Samples of the electrolyte were collected and analyzed before and after electrolysis. Additional CO_2 was bubbled directly into the working compartment through a gas dispersion tube (Ace Glass, d= 7 mm) at a rate of 10 mL/min controlled by a mass flow controller (MFC). A schematic of the cell setup is described elsewhere[32].

Headspace gas was vented directly to a gas chromatograph (GC, 7890A, Agilent Technologies) equipped with a mass spectrometer (MS) and a thermal conductivity detector (TCD), details of the two-column setup is described elsewhere[32]. 10 uL of the gas aliquots are injected automatically to the GCMS and GCTCD every 7-10 minutes. Gas flow rate into the electrochemical cell was controlled by the MFC. The combined CO_2 and gas flow rate was measured at the end of the sample loop by a soap-bubble flow meter (Model 520, Fischer Scientific).

3.4 Electrolysis and Product Analysis

Electrolysis experiments were performed at -1.35 V vs. $RHE_{pH6.8}$. The electrochemical cell was run as a flow reactor and gaseous products were collected continuously, while the liquid product was collected at the end of 30 minutes when the electrolyte flow was stopped. The electrolysis prior to analyte injection is done to allow both the surface and CO_2 products to reach an equilibrium. At this point, the flow and applied potential was stopped and 1 mL of 2500 ppm (0.0567 M) or 5000 ppm (0.114 M) acetaldehyde or propionaldehyde was injected through the top port of the working electrode compartment via syringe. The electrolysis cell was then operated under a batch reaction configuration (fresh electrolyte flow was stopped into the electrode compartments and the outward flow from the working electrode was also stopped). Gaseous products were measured from the headspace using a GCMS/GCTCD every 7 minutes. Electrolysis

continued under batch conditions for 30 minutes and the liquid contents of the working electrode compartment were collected in scintillation vials. These vials were placed in the refrigerator immediately to minimize loss of volatile compounds. The solution from the counter electrode compartment was also collected to verify that no liquid products had leaked across the membrane from the working electrode compartment. Liquid products were analyzed using an AVIII 400 MHz NMR spectrometer. NMR samples were prepared with 0.8 mL of collected sample, 0.1 mL of D_2O, and 0.1 mL of 100 ppm acetonitrile, as an internal standard. A water suppression method was used for ^{1}H NMR analysis. ^{13}C NMR was used for carbon analysis.

Isotopic studies were conducted by replacing the reactant with the ^{13}C enriched equivalent. In these experiments, ^{13}C labelled acetaldehyde and $^{13}CH_3{}^{13}COH$ (Sigma-Aldrich, 99%), where both carbons are labelled, was used. A reference NMR spectrum was obtained of a labelled acetaldehyde in a 0.1 M $KHCO_3$ solution for reference chemical shifts and splitting patterns (Figure 2).

Faradaic efficiencies (FE) were calculated using equation 2, by counting the electrons required to produce each species from CO_2 in the given time period and comparing that to the total electrons passed in that same time period and reporting the efficiency as a percentage. The rate of formation was calculated based on the moles of products produced, obtained from the quantitative analysis of the products over a period of time and normalized to the geometric area of the catalyst (equation 3).

$$FE\ (\%) = Q_{products}/Q_{total} \times 100 \qquad (2)$$

Rate of formation (mol/cm^2-sec)

= molProduct/1800 sec /26 cm^2 (3)

4. Results and Discussion

First, in an aqueous solution at room temperature, aldehydes exist as an equilibrium mixture with their diols. For example, acetaldehyde and ethanediol are typically in a 0.8:1.0 ratio with an equilibrium constant, K = 1.246 at 20 ºC. The rate constant of hydration has been reported to be 9.0 x 10^{-3} s^{-1} at 25 ºC[33]. The splitting pattern of the equilibrium mixture can easily be observed in the ^{1}H-NMR and ^{13}C-NMR obtained from a 2500 ppm (0.0567 M) solution of acetaldehyde in 0.1 M $KHCO_3$ (Figure 2). In describing the experimental work, we will use the name acetaldehyde to refer to both the carbonyl and hydrated form and will not attempt to differentiate whether ethanol is formed from acetaldehyde or ethanediol. This also applies to the three-carbon aldehyde, propanal, shown to be at equilibrium with propanediol (Figure 2). DFT calculations discussed briefly in the latter part of this paper will address and suggest the likelihood of acetaldehyde reduction to ethanol, as opposed to ethanediol reduction.

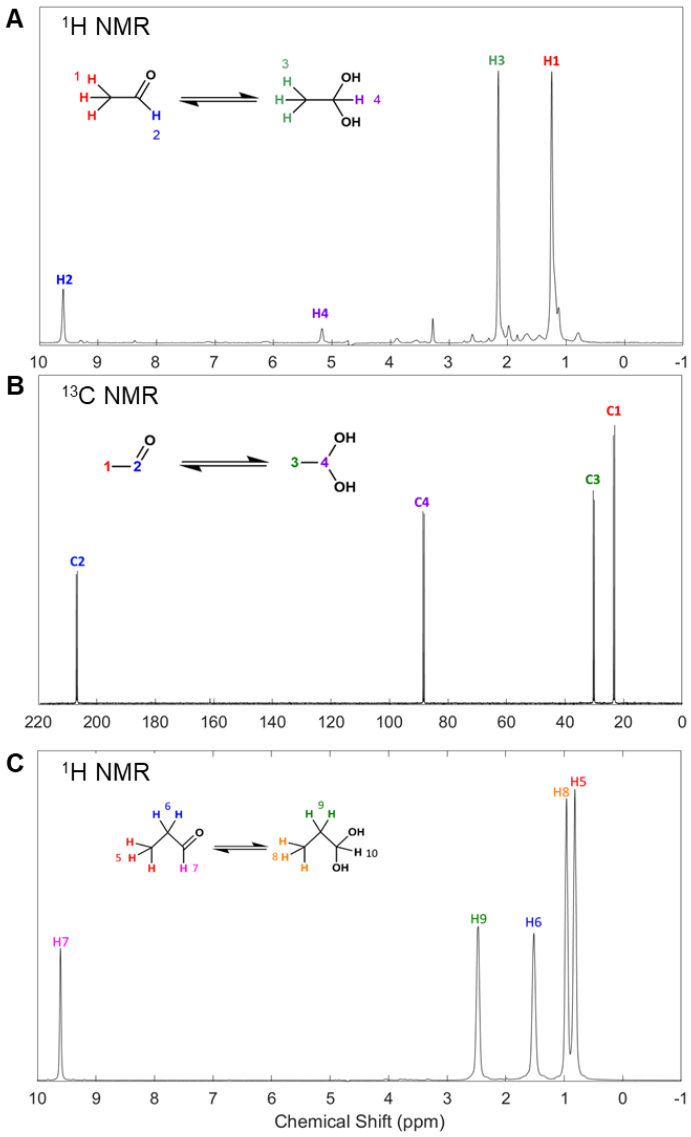

Figure 2. (A) ^{1}H NMR spectra of 2500 ppm (0.0567 M) acetaldehyde in 0.1 M $KHCO_3$. 128 scans using a water suppression method on a 400 MHz NMR. (B) ^{13}C NMR spectra of 2500 ppm (0.0567 M) acetaldehyde in 0.1 M $KHCO_3$. 512 scans on 400 MHz Bruker NMR. (C) ^{1}H NMR spectra of 5000 ppm (0.114 M) propanal in 0.1 M $KHCO_3$. 128 scans with a water suppression method on a 400 MHz Bruker NMR.

A freshly electropolished and cleaned Cu foil electrode is assembled in an electrochemical flow cell as described in the experimental and elsewhere[32]. A baseline product distribution from the electrolysis of CO_2 at –1.35 V vs. $RHE_{6.8}$ (ca. 0.003 mA/cm^2) was obtained after steady state is achieved, approximately 30 min after electrolysis. The rate of formation and the corresponding Faradaic efficiency of the products detected are tabulated in Table 2. After which, a 2500 ppm (0.0567 M) solution of acetaldehyde (non-isotopically labeled) was injected in the electrochemical cell and reduced for another 30 minutes in a batch reaction configuration (Table 3). Liquid products were collected and analyzed by NMR. The solution in the counter electrode compartment was also routinely collected and tested to verify that no reactants or products from the working electrode compartment is crossing the ion exchange membrane.

Table 2. Faradaic efficiencies and the rate of formation for the production of each observed species in the reduction of CO_2 on electropolished copper in 0.1 M $KHCO_3$ at -1.35 V vs RHE after 30 minutes.

Product	Faradaic Efficiency (without additional acetaldehyde)	Rate of Formation (mol/sec*cm^2)
H_2	58% ± 10%	$1.5*10^{-9}$
CO	1.3% ± 0.2%	$3.1*10^{-11}$
CH_4	11% ± 3%	$6.4*10^{-11}$

C_2H_4	9% ± 2%	$3.3*10^{-11}$
HCO_2^-	6.72% ± 0.2%	$1.2*10^{-9}$
C_2H_4OH	4% ± 1.5%	$1.2*10^{-10}$

*Error reported from standard deviation calculations based on replication of the full electrolysis experiment

Table 3. Faradaic efficiencies and the rate of formation for the production of each observed species in the reduction of CO_2 and 2500 ppm (0.0567 M) acetaldehyde on electropolished copper in 0.1 M $KHCO_3$ at -1.35 V vs RHE <u>after 30 minutes</u>.

Product	Faradaic Efficiency with addition of acetaldehyde	Rate of Formation (mol/sec*cm^2)
H_2	57% ± 10%	1.5×10^{-9}
CO	1.3%*	3.1×10^{-11}
CH_4	11%*	6.4×10^{-11}
C_2H_4	9%*	3.3×10^{-11}
HCO_2^-	4%*	1.2×10^{-9}

C_2H_4OH	7%*	6.5 x 10^{-10}
Acetaldehyde consumed	0.024 mmol	
C_2H_4OH from acetaldehyde	0.022 mmol (92 % conversion)	5.3*10^{-10}

* Error < 3%

*Error reported from standard deviation calculations based on replication of the full electrolysis experiment

It is apparent that there was significantly more ethanol produced in the batch reaction after acetaldehyde was added to the reduction cell. Stoichiometric calculations showed that there was a correlation between the amount of ethanol produced and the amount of acetaldehyde consumed (Figure 3A-D). The Faradaic efficiency of a 2-electron reduction process of acetaldehyde to ethanol is around 92%.

To further verify that ethanol was produced from the reduction of acetaldehyde, the experiment was also reproduced with an isotopically labeled acetaldehyde solution (both carbons are labelled with ^{13}C). The ^{13}C NMR and ^{1}H NMR splitting patterns of the labelled carbons in ethanol supports that this additional ethanol was derived solely from the labelled aldehydes. Based on these results, it can be established that the aldehyde functional group can be electrochemically reduced to alcohols. We also observed this for a three-carbon aldehyde. Figure 3E show the electrochemical

reduction of propionaldehyde results in 1-propanol. While isotopic studies of propanal were not conducted at this time, quantification by ^{1}H NMR, in water suppression mode, does provide strong evidence that propanol was derived from the reduction of propanal. As acetaldehyde and propanal are sometimes observed as trace amounts in the CO_2 and CO reduction processes[8,30], evidence shown in this study strongly supports that these aldehyde species are very likely intermediates that can be further reduced to form the primary alcohols.

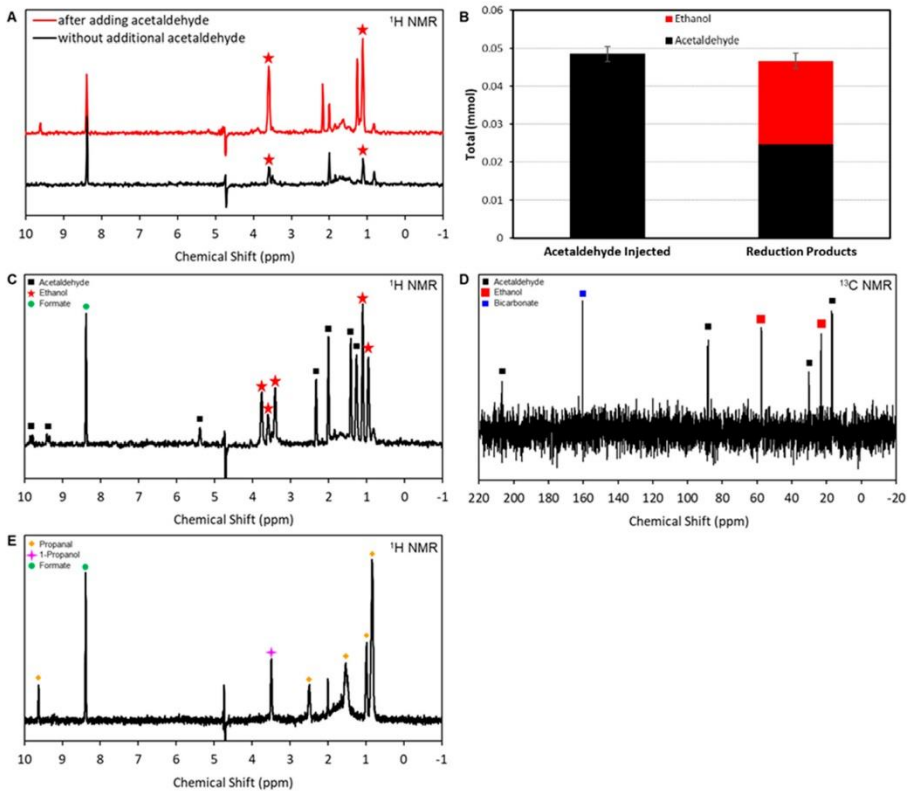

Figure 3. (A) ^{1}H NMR spectra of the aqueous products of CO_2 reduction on electropolished copper in 0.1M $KHCO_3$ with and without injection of 2500 ppm (0.0567 M) acetaldehyde. Reduction performed at -1.35 V (vs. RHE). Ethanol peaks are indicated with the star symbol. (B) Graphical display of the added and the additional ethanol produced from the electroreduction of acetaldehyde. Mole amounts were calculated from ^{1}H NMR peak integration compared to standard calibration plots. (C) ^{1}H NMR and (D) ^{13}C NMR spectra of the aqueous products of CO_2 reduction on electropolished copper in 0.1 M $KHCO_3$ after the addition of ^{13}C acetaldehyde. Reduction performed at -1.35 V (vs. RHE). The presence of ^{13}C ethanol provides conclusive evidence that the acetaldehyde injected is being converted to the observed ethanol. (E) ^{1}H NMR spectra of the aqueous products of CO_2 reduction on electropolished copper in 0.1 M $KHCO_3$ after the addition of propanal. Reduction performed at -1.35 V (vs. RHE). The appearance of 1-propanol provides evidence of propanal conversion to prop

It follows logically to question whether Cu is unique in its ability catalyze the reduction of small aldehydes to primary alcohols compared to other catalysts often used in CO2RR. In this study, Au was also tested to see if it could reduce aldehydes to alcohols. It has been reported in the past that Au produces almost exclusively CO[34,35] during CO_2 reduction and that other hydrocarbons are not commonly observed. Here, an Au film was prepared by sputtering approx. 100-200 nm of Au on stainless steel (8 cm x 4.5 cm) and cut to fit in the same electrochemical cell. Experimental procedure, similar to those described earlier, was conducted using Au catalyst. First, CO_2 reduction was conducted on Au and produced mainly CO. Acetaldehyde was then injected into the electrochemical cell held at -1.35 V vs. $RHE_{pH6.8}$, where no ethanol nor any additional products were observed (Figure 4A)

Additionally, chemical catalysis of acetaldehyde to ethanol was also investigated. The ^1H NMR in Figure 4B is an example demonstrating that without applying an external voltage to drive the reaction, Cu is inactive towards the catalysis of acetaldehyde, even at elevated temperatures of 100 ^oC.

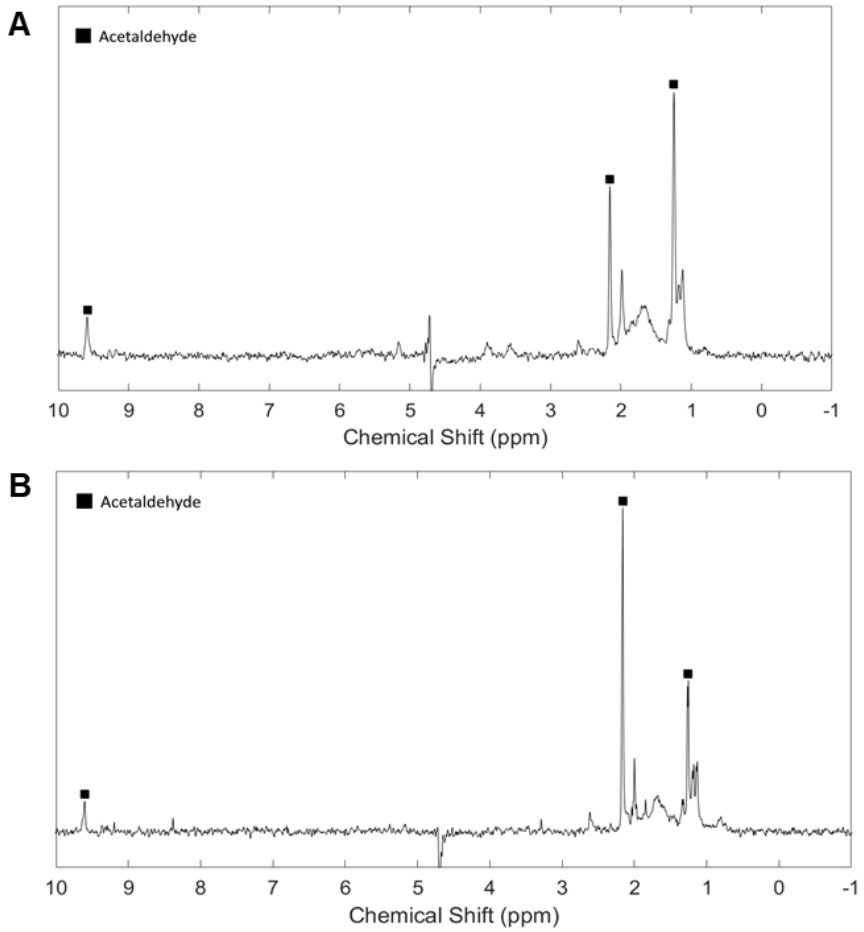

Figure 4. (A) ^{1}H NMR spectra of the aqueous products of CO_2 reduction on (a) Au sputtered stainless steel in 0.1 M $KHCO_3$ with the acetaldehyde added to the solution. Reduction performed at -1.35 V (vs. RHE), and (B) polycrystalline copper in 0.1 M $KHCO_3$ with acetaldehyde added to the solution. Reaction conducted at 100 ^{o}C for at least 30 min, with no applied potential.

5. Theoretical Calculations

A number of questions remained open following the experimental study, namely which form of the aldehyde proceeds through the reaction and whether a reasonable argument can be provided for the inability of gold to catalyze the reduction of aldehydes to alcohols. Zhihao Cui of the Co group performed Density Functional theory calculations using the Vienna Ab-Initio Simulation Package to provide answers to both of these questions[36].

In regard to the diol or aldehyde as the primary species being reduced on the surface to the alcohol, calculations show a lower barrier to reaction when proceeding through the aldehyde

and as such this is likely to be the species which participates. Analysis of gold's ability to catalyze the reaction shows a substantially higher reaction barrier than on copper which may be causal for why gold is incapable of catalyzing this reaction.

6. Conclusion

This study shows that aldehydes can be electrochemically reduced to alcohol. This was demonstrated for acetaldehyde reduction to ethanol and propanal reduction to 1-propanol. Both acetaldehyde and propanal form hydrated species at equilibrium with the aldehyde in aqueous solution at room temperature. While 1,1-ethanediol along with acetaldehyde can be detected in the ^{1}H NMR, it is experimentally challenging to identify the species involved in the reduction. DFT calculations utilizing the computational hydrogen electrode model suggest favorable dissociation of ethanediol to acetaldehyde and water on Cu(100), where the protonation of η(O,O)-$CH_3CH(OH)_2$* is less favorable on Cu(100) and the dissociation of η(O,O)-$CH_3CH(OH)_2$* into η(O)-CH_3CH_2O* and H_2O* is a preferred pathway due to a relatively low reaction free energy. The calculations also suggest that the pathway of acetaldehyde to ethanol goes through η(O)-CH_3CH_2O* instead of η(C)-CH_3CHOH* intermediate on Cu(100).

Experiments confirm high selectivity and conversion efficiency on Cu, whereas the electroreduction does not occur on Au. DFT calculation supports this observation. The calculated activation energy and reaction free energy of the protonation of η(O,O)-$CH_3CH(OH)_2$* suggest that acetaldehyde can hardly be reduced to ethanol on Au(111), even though the dissociation of η(O,O)-$CH_3CH(OH)_2$* into η(O)-CH_3CH_2O* and H_2O* is thermodynamically favorable on Au(111).

The reduction of aldehydes to alcohols is a plausible intermediate step in the overall mechanistic pathway of converting CO_2 to alcohols. Investigating the electrochemical reduction of aldehydes to alcohols provides insights into the mechanism. In this work, we reveal that while the reaction step involving the reduction of aldehyde may not be the limiting step in the overall reduction of CO_2, the selective reduction observed on Cu suggests that the role and effect of a catalysts, especially for complex multistep reactions, may be more involved beyond affecting the slowest step. In summary, the results from this study supports previously proposed mechanisms and may provide a framework for testing other stable CO_2 reaction intermediates in the future to gain insights to the overall CO_2 reaction pathway.

7. Future Work

Several challenges still exist within the framework of the experiments described herein before even considering the development of an advanced catalyst. The first experiments will seek to eliminate catalyst poisoning as a possible explanation for the lack of catalytic activity on gold. Additional insights may be gained by analyzing onset potentials of the different aldehyde reductions. Finally, a singly labeled aldehyde (only one carbon-13) may provide deeper insight to reaction intermediates.

8. Bibliography

(1) US Department of Commerce, N. Global Monitoring Laboratory - Carbon Cycle Greenhouse Gases https://www.esrl.noaa.gov/gmd/ccgg/trends/ (accessed Oct 17, 2020).

(2) *Lange's Handbook of Chemistry*, 15. ed.; Dean, J. A., Lange, N. A., Eds.; McGraw-Hill handbooks; McGraw-Hill: New York, NY, 1999.

(3) Electrochemical Energy Systems https://ocw.mit.edu/courses/chemical-engineering/10-626-electrochemical-energy-systems-spring-2014/ (accessed Apr 13, 2021).

(4) Lund, H. Renewable Energy Strategies for Sustainable Development. *Energy* **2007**, *32* (6), 912.

(5) Kuhl, K. P.; Cave, E. R.; Abram, D. N.; Jaramillo, T. F. New Insights into the Electrochemical Reduction of Carbon Dioxide on Metallic Copper Surfaces. *Energy Env. Sci* **2012**, *5* (5), 7050.

(6) Gattrell, M.; Gupta, N.; Co, A. A Review of the Aqueous Electrochemical Reduction of CO2 to Hydrocarbons at Copper. *J. Electroanal. Chem.* **2006**, *594* (1), 1–19. https://doi.org/10.1016/j.jelechem.2006.05.013.

(7) Gattrell, M.; Gupta, N.; Co, A. Electrochemical Reduction of CO2 to Hydrocarbons to Store Renewable Electrical Energy and Upgrade Biogas. *Energy Convers Manage* **2007**, *48* (4), 1255.

(8) Chang, Z. Y.; Huo, S. J.; Zhang, W.; Fang, J. H.; Wang, H. L. The Tunable and Highly Selective Reduction Products on Ag@Cu Bimetallic Catalysts Toward CO2 Electrochemical Reduction Reaction. *J Phys Chem C* **2017**, *121* (21), 11368.

(9) Hori, Y.; Vayenas, C. G.; White, R. E.; Gamboa-Aldeco, M. E. *Modern Aspects of Electrochemistry*; 2008.

(10) Hori, Y.; Murata, A.; Takahashi, R. Formation of Hydrocarbons in the Electrochemical Reduction of Carbon-Dioxide at a Copper Electrode in Aqueous-Solution. *J Chem Soc Faraday Trans 1* **1989**, *85*, 2309.

(11) Schouten, K. J. P.; Calle-Vallejo, F.; Koper, M. T. M. A Step Closer to the Electrochemical Production of Liquid Fuels. *Angew Chem Int Ed* **2014**, *53* (41), 10858.

(12) Schouten, K. J. P.; Gallent, E. P.; Koper, M. T. M. The Influence of PH on the Reduction of CO and CO2 to Hydrocarbons on Copper Electrodes. *J Electroanal Chem* **2014**, *716*, 53.

(13) Reske, R.; Duca, M.; Oezaslan, M.; Schouten, K. J. P.; Koper, M. T. M.; Strasser, P. Controlling Catalytic Selectivities during CO2 Electroreduction on Thin Cu Metal Overlayers. *J Phys Chem Lett* **2013**, *4* (15), 2410.

(14) Schouten, K. J.; Koper, M.; Lewerenz, H. J.; Peter, L. *Photoelectrochemical Water Splitting: Materials, Processes and Architectures*; 2013.

(15) Schouten, K. J. P.; Qin, Z. S.; Gallent, E. P.; Koper, M. T. M. Two Pathways for the Formation of Ethylene in CO Reduction on Single-Crystal Copper Electrodes. *J Am Chem Soc* **2012**, *134* (24), 9864.

(16) Garza, A. J.; Bell, A. T.; Head-Gordon, M. Mechanism of CO2 Reduction at Copper Surfaces: Pathways to C2 Products. *ACS Catal.* **2018**, *8* (2), 1490–1499. https://doi.org/10.1021/acscatal.7b03477.

(17) Garza, A. J.; Bell, A. T.; Head-Gordon, M. Is Subsurface Oxygen Necessary for the Electrochemical Reduction of CO2 on Copper? *J Phys Chem Lett* **2018**, *9* (3), 601.

(18) Nitopi, S.; Bertheussen, E.; Scott, S. B.; Liu, X. Y.; Engstfeld, A. K.; Horch, S.; Seger, B.; Stephens, I. E. L.; Chan, K.; Hahn, C.; Norskov, J. K.; Jaramillo, T. F.; Chorkendorff, I. Progress and Perspectives of Electrochemical CO2 Reduction on Copper in Aqueous Electrolyte. *Chem Rev* **2019**, *119* (12), 7610.
(19) Singh, M. R.; Goodpaster, J. D.; Weber, A. Z.; Head-Gordon, M.; Bell, A. T. Mechanistic Insights into Electrochemical Reduction of CO2 over Ag Using Density Functional Theory and Transport Models. *Proc Natl Acad Sci U A* **2017**, *114* (42), E8812.
(20) Goodpaster, J. D.; Bell, A. T.; Head-Gordon, M. Identification of Possible Pathways for C–C Bond Formation during Electrochemical Reduction of CO2: New Theoretical Insights from an Improved Electrochemical Model. *J. Phys. Chem. Lett.* **2016**, *7* (8), 1471–1477. https://doi.org/10.1021/acs.jpclett.6b00358.
(21) Montoya, J. H.; Peterson, A. A.; Norskov, J. K. Insights into CC Coupling in CO2 Electroreduction on Copper Electrodes. *ChemCatChem* **2013**, *5* (3), 737.
(22) Peterson, A. A.; Abild-Pedersen, F.; Studt, F.; Rossmeisl, J.; Norskov, J. K. How Copper Catalyzes the Electroreduction of Carbon Dioxide into Hydrocarbon Fuels. *Energy Env. Sci* **2010**, *3* (9), 1311.
(23) Hori, Y.; Takahashi, R.; Yoshinami, Y.; Murata, A. Electrochemical Reduction of CO at a Copper Electrode. *J Phys Chem B* **1997**, *101* (36), 7075.
(24) Garza, A. J.; Bell, A. T.; Head-Gordon, M. Mechanism of CO2 Reduction at Copper Surfaces: Pathways to C2 Products. *ACS Catal.* **2018**, *8* (2), 1490–1499. https://doi.org/10.1021/acscatal.7b03477.
(25) Montoya, J. H.; Shi, C.; Chan, K.; Norskov, J. K. Theoretical Insights into a CO Dimerization Mechanism in CO2 Electroreduction. *J Phys Chem Lett* **2015**, *6* (11), 2032.
(26) Chang, X.; Malkani, A.; Yang, X.; Xu, B. Mechanistic Insights into Electroreductive C–C Coupling between CO and Acetaldehyde into Multicarbon Products. *J Am Chem Soc* **2020**, *142* (6), 2975.
(27) Calle-Vallejo, F.; Koper, M. T. M. Theoretical Considerations on the Electroreduction of CO to C-2 Species on Cu(100) Electrodes. *Angew Chem Int Ed* **2013**, *52* (28), 7282.
(28) Luo, W.; Nie, X.; Janik, M. J.; Asthagiri, A. Facet Dependence of CO2 Reduction Paths on Cu Electrodes. *ACS Catal.* **2016**, *6* (1), 219–229. https://doi.org/10.1021/acscatal.5b01967.
(29) Schouten, K. J. P.; Kwon, Y.; van der Ham, C. J. M.; Qin, Z.; Koper, M. T. M. A New Mechanism for the Selectivity to C-1 and C-2 Species in the Electrochemical Reduction of Carbon Dioxide on Copper Electrodes. *Chem Sci* **2011**, *2* (10), 1902.
(30) Bertheussen, E.; Verdaguer-Casadevall, A.; Ravasio, D.; Montoya, J. H.; Trimarco, D. B.; Roy, C.; Meier, S.; Wendland, J.; Nørskov, J. K.; Stephens, I. E. L.; Chorkendorff, I. Acetaldehyde as an Intermediate in the Electroreduction of Carbon Monoxide to Ethanol on Oxide-Derived Copper. *Angew Chem Int Ed* **2016**, *55* (4), 1450.
(31) Ledezma-Yanez, I.; Gallent, E. P.; Koper, M. T. M.; Calle-Vallejo, F. Structure-Sensitive Electroreduction of Acetaldehyde to Ethanol on Copper and Its Mechanistic Implications for CO and CO2 Reduction. *Catal Today* **2016**, *262*, 90.
(32) Billy, J. T.; Co, A. C. Experimental Parameters Influencing Hydrocarbon Selectivity during the Electrochemical Conversion of CO_2. *ACS Catal.* **2017**, *7* (12), 8467–8479. https://doi.org/10.1021/acscatal.7b02373.
(33) Kurz, J. L. HYDRATION OF ACETALDEHYDE. I. EQUILIBRIUM THERMODYNAMIC PARAMETERS. *J Am Chem Soc* **1967**, *89* (14), 3524.

(34) Cave, E. R.; Montoya, J. H.; Kuhl, K. P.; Abram, D. N.; Hatsukade, T.; Shi, C.; Hahn, C.; Norskov, J. K.; Jaramillo, T. F. Electrochemical CO2 Reduction on Au Surfaces: Mechanistic Aspects Regarding the Formation of Major and Minor Products. *Phys Chem Chem Phys* **2017**, *19* (24), 15856.
(35) Wuttig, A.; Yaguchi, M.; Motobayashi, K.; Osawa, M.; Surendranath, Y. Inhibited Proton Transfer Enhances Au-Catalyzed CO2-to-Fuels Selectivity. *Proc. Natl. Acad. Sci.* **2016**, *113* (32), E4585–E4593. https://doi.org/10.1073/pnas.1602984113.
(36) Charnay, B. P.; Cui, Z.; Marx, M. A.; Palazzo, J.; Co, A. C. Insights into the CO2 Reduction Pathway through the Electrolysis of Aldehydes on Copper. *ACS Catal.* **2021**, 3867–3876. https://doi.org/10.1021/acscatal.0c05615.